HHS Public Access

Author manuscript

Pain. Author manuscript; available in PMC 2024 August 01.

Published in final edited form as:

Pain. 2023 August 01; 164(8): 1874–1886. doi:10.1097/j.pain.0000000000002889.

Peripheral TRPV4 hypersensitivity contributes to chronic sickle cell disease pain

Vanessa L. Ehlers[1], **Katelyn E. Sadler**[1], **Cheryl L. Stucky**[1]

[1]Department of Cell Biology, Neurobiology and Anatomy, Medical College of Wisconsin, Milwaukee WI

1. Introduction

Individuals with sickle cell disease (SCD) experience debilitating pain that severely diminishes quality of life. In SCD, a single point mutation in the β-hemoglobin gene triggers hemoglobin polymerization, giving rise to the characteristic sickle shape of red blood cells. This contributes to blockade of blood vessels and triggers vaso-occlusive crises (VOCs)[46,78]. In addition to these acute pain episodes, nearly 30% of patients with SCD will develop daily chronic pain[98], the underlying causes of which are still poorly understood. Two transgenic mouse models, the Berkeley and Townes models, are useful for examining the neurobiological basis of chronic SCD pain[76,85]. These mouse models consistently demonstrate behavioral hypersensitivity to mechanical and thermal stimuli[18–20,41,53,54,87,89,91,112], and demonstrate peripheral nerve fiber dysfunction[11,33,39,41,43,49–51,66,77,87,88,91,113,114,118]. The transient receptor potential (TRP) family of ion channels are expressed in mouse and human peripheral tissues[90,97,108] where they regulate several processes required for normal somatosensation, including osmosensation[64,102] and mechanosensation[103]. Several TRP channels have previously been shown to contribute to hypersensitivity in SCD[41,89], however, the pathophysiology of the disease suggests that more family members may be involved in this process.

TRPV4 is implicated in pathological pain conditions that have hallmarks similar to SCD, including tissue inflammation[4,5,9,22–24,99,121,122] and neuropathy[6,7,67,68,120], as well as in hypo- and hypertonicity-mediated nociception[8,9]. TRPV4 is highly expressed in rodent dorsal root ganglia (DRG) neurons[9,65,92], and in human DRG neurons TRPV4 is primarily expressed in Aβ and silent nociceptors[108]. TRPV4 is also highly expressed in keratinocytes[23,25,36,83,94,100,104], the primary cell type of the epidermis which were recently shown to be critical modulators of primary sensory afferent activity[14,70,75]. Notably, keratinocyte-expressed TRPV4 activity is required for UV-burn related mechanical

Corresponding Author: Cheryl Stucky, PhD; 8701 Watertown Plank Road, Milwaukee WI 53226; cstucky@mcw.edu; 414-955-8373; https://www.mcw.edu/.

Author Contributions: V.L. Ehlers and K.E. Sadler and C.L. Stucky designed the experiments; K.E. Sadler collected and analyzed the behavior data; V.L. Ehlers collected and analyzed the patch clamp and calcium imaging data; V.L. Ehlers wrote the manuscript; V.L. Ehlers, K.E. Sadler, and C.L. Stucky edited the manuscript.

Conflict of Interest Statement

The authors have no conflict of interest to declare.

allodynia[72], further suggesting that peripheral non-neuronal expression of this channel is also important for inflammatory pain conditions. Despite all this, TRPV4 remains an unexplored candidate mechanism in the hyperalgesia characteristic of SCD. In the present study we examined whether TRPV4 mediates behavioral and cellular sensitization in SCD mice using a combination of evoked behavior assays, patch clamp recordings, and calcium imaging. These experiments are the first to investigate a functional role for TRPV4 in SCD hypersensitivity.

2. Methods

2.1. Animals

Two transgenic SCD mouse lines, Berkeley and Townes, were used in the current experiments. Berkeley sickle cell (Berk SS) mice have murine α and β hemoglobin genes knocked out and human α globin and sickle β globin genes are expressed using a transgene [Tg(Hu-miniLCRα1$^{G}\gamma^{A}\gamma\delta\beta^{S}$)][76]. Because the Berkeley genetic background comes from C57BL/6 and 129 mice, B6/129 hybrid mice were used as a wildtype (WT) control for Berk SS mice. Townes murine *Hba* and *Hbb* genes are knocked out and human *HBA* and sickle *HBB* genes are knocked in at the same locus (Townes SS); WT control Townes mice contain human *HBA* and normal *HBB* genes (Townes AA) [85]. Both Berk SS and Townes SS mouse models are homozygous for sickle β globin, leading to pathology like that seen in SCD patients. These mouse models also display many of the same characteristics of human patients with SCD, including persistent hypersensitivity to mechanical and cold stimuli[15,47]. Equivalent numbers of male and female mice were used for all experiments. Ages ranged from 12-56 weeks. All mice were bred and maintained in a climate-controlled room on a 14:10 light/dark cycle and given free access to food and water. Mice were group housed by genotype. All protocols were in accordance with National Institutes of Health guidelines and were approved by the Institutional Animal Care and Use Committee at the Medical College of Wisconsin (Milwaukee, WI; protocol 383).

2.2. Behavior

For all behavioral testing, Townes AA (WT) and Townes SS (SCD) mice were habituated to test chamber and experimenter for >1 h[101], and all mice were randomly assigned to treatment groups. Given that the selective TRPV4 inhibitor GSK2193874 reduces osteoarthritic pain behavior and spontaneous DRG action potential firing at 1μM[99], mice received intraplantar injections of 20 μL of PBS (vehicle) or GSK2193874 (TRPV4 antagonist; Tocris Bioscience) at 30, 100, or 300 nM concentrations. Behavioral testing began 45 min after injection.

2.2.1. Mechanical sensitivity—The von Frey up-down assay was used to examine sensitivity to punctate mechanical stimuli. Calibrated filaments (0.2-13.73 mN) were used to calculate a 50% withdrawal threshold for each paw, as previously described[21,29]. If toe flaring occurred without paw withdrawal, it was not considered a response.

Noxious needle testing was performed to assess hind paw sensitivity to noxious punctate mechanical stimuli as previously described[42]. Each paw was stimulated 10 times by

pressing a 25-gauge spinal needle into the center of each hind paw to indent the skin but not puncture it. Response frequency was recorded and characterized as either null (no paw withdrawal), normal (simple withdrawal) or nocifensive (withdrawal accompanied by biting, licking, flicking, or additional hind paw attending).

Paintbrush stimulation was used to determine the extent of hind paw sensitivity to dynamic light touch as previously described[26]. Each paw was stimulated 10 times by sweeping a fine horsehair paintbrush across the plantar skin from heel to toe pads and maintaining approximately consistent speed and force between applications. Like needle testing, response frequency and characterization (null, normal, nocifensive) were recorded.

2.2.2. Cold sensitivity—To test sensitivity to noxious cold as previously described[16], powdered dry ice was packed into a 3 mL plastic syringe with the tip removed. The dry ice was applied to the underside of a 1/4 inch thick Plexiglas floor, underneath each plantar hind paw, for no more than 20 s per stimulation. Each paw was stimulated 4 times. Withdrawal latencies recorded for each paw were averaged together for each animal.

2.3. Cell culture

2.3.1. Dorsal root ganglia (DRG) neurons—Under deep isoflurane anesthesia, mice were euthanized through decapitation. Bilateral lumbar 1-6 DRG were dissected and collected in HBSS+Ca^{2+}, then incubated in Ham's DMEM/F12 medium with 10mg/mL collagenase type IV for 40 min, then 0.05% trypsin for 45 min at 37°C in 5% CO_2. Mechanical trituration was used to physically dissociate cells, which were then plated onto laminin-coated glass coverslips. Coverslips were incubated for 1-2 h before flooding the wells with media (Ham's F12 supplemented with 10% heat-inactivated horse serum, 1% glucose, 100 units/mL penicillin, and 100 μg/mL streptomycin, 2 mM L-glutamine), and were then incubated overnight. For calcium imaging experiments, cells were additionally centrifuged at 2800rpm for 1 min, supernatant removed and 1mL DMEM/F12 media added before incubation in trypsin. A similar centrifugation step was added immediately before cells were plated onto coverslips.

2.3.2. Keratinocytes—Under deep isoflurane anesthesia, mice were euthanized through cervical dislocation. Glabrous skin of the mouse hind paw was dissected and incubated in 20 mg/mL dispase for 45 min at room temperature (RT). Epidermal and dermal layers were then separated, and the epidermis was incubated in 50% EDTA and 0.05% trypsin in HBSS without calcium chloride, magnesium chloride, and magnesium sulfate for 27 min at RT. Following exposure to 15% heat inactivated fetal bovine serum, epidermal sheets were rubbed against the base of a petri dish to dissociate the tissue. The resulting solution (consisting primarily of single keratinocytes) was centrifuged, supernatant was removed, and the pellet was resuspended in Epilife media with 1% human keratinocyte growth supplement, Amphotericin B (250μg/mL Amphotericin B and 205 μg/mL sodium deoxycholate), and 0.25% penicillin-streptomycin. Cells were plated on laminin-coated coverslips and incubated at 37°C and 5% CO_2. Forty-eight hours after initial plating, cell media was exchanged. Keratinocytes were used for calcium imaging experiments 3-4 days after plating.

2.4. Calcium imaging

Calcium imaging experiments were performed on DRG neurons isolated from B6;129 (WT) and Berkeley SS (SCD) mice following overnight culture. Coverslips were incubated in 2.5 μg/mL Fura-2-AM (a dual-wavelength ratiometric calcium indicator dye) in 2% bovine serum albumin for 45 min, followed by a 30 min wash in extracellular normal HEPES buffer (ENH) before imaging. Coverslips were mounted on a Nikon Eclipse TE200 inverted microscope and were superfused with RT ENH (pH 7.4 ± 0.03; 320 ± 3 mOsm; in mM: 150 NaCl • 10 HEPES • 8 glucose • 5.6 KCl • 2 $CaCl_2$ • 1 $MgCl_2$). Fluorescence images were obtained at 340 and 380 nm using Nikon Elements software (Nikon Instruments, Melville, NY). Based on previous research showing mouse DRG neuron calcium responses to the TRPV4 agonist GSK1016790A increase in a concentration-dependent manner up to 1000nM[10], GSK1016790A was superfused at 30, 100, 300 or 1000 nM concentrations (made from serial dilutions) in the present study. Following a 1 min baseline incubation in ENH, DRG neurons were incubated in GSK1016790A for 2 min, ENH for 3 min, and 50 mM KCl for 1 min. All buffers were superfused at a rate of 6 mL/min. DRG neurons were included for response magnitude analysis if they displayed a ≥20% increase in the 340/380 nm ratio relative to baseline in response to GSK1016790A or KCl. Analyses of small soma diameter (<27μm) and large diameter (≥27μm) neurons were conducted separately.

Keratinocytes from Townes AA (WT) and Townes SS (SCD) mice underwent calcium imaging on days 3-4 in culture. Like DRG neurons, keratinocyte coverslips were incubated in 2.5 μg/mL Fura-2-AM for 45 min, then coverslips were washed with ENH for 30 min before imaging. A 1 min ENH baseline was followed by 3 min application of GSK1016790a (1, 3, 6 or 10nM), with a 6 min ENH wash. Buffers were superfused at 6 mL/min. For all calcium imaging experiments using keratinocytes, cells were included for response magnitude analysis if they displayed a ≥30% increase in the 340/380 nm ratio relative to baseline in response to GSK1016790a.

2.5. Patch clamp electrophysiology

Whole-cell patch clamp recordings of DRG neurons were obtained from Townes AA (WT) or Townes SS (SCD) mice following overnight culture. Coverslips were mounted on an inverted Nikon Eclipse TE200 microscope, and continuously superfused with RT ENH (pH 7.4 ± 0.03; 310 ± 3 mOsm; in mM: 140 NaCl • 2.8 KCl • 2 $CaCl_2$ • 1 $MgCl_2$ • 10 HEPES • 10 glucose • 8.8 sucrose) or ENH containing 300nM of the TRPV4 inhibitor GSK2193874. Patch clamp recordings of DRG neurons (held at −70 mV) were obtained using borosilicate glass pipettes filled with intracellular normal HEPES buffer (pH: 7.2 ± 0.02; 290 ± 3 mOsm; in mM: 135 KCl • 4.1 $MgCl_2$ • 2 EGTA • 0.2 mM NaGTP • 2.5 mM $ATPNa_2$ • 10 mM HEPES), pulled using a Sutter Instruments P87 pipette puller. A second borosilicate glass pipette driven by a piezo stack actuator was used for cell membrane mechanical displacement. Series resistance was compensated at 60% and kept ≤10 MΩ. Recordings were obtained using a HEKA EPC10 amplifier and HEKA Patchmaster Next software. Signals were filtered at 2.9 kHz and digitized at 10 kHz. Neuronal capacitance was continuously monitored to ensure stable recording conditions, and neurons were excluded from data collection if resting membrane potential (RMP) > −40mV.

Current-voltage relations were obtained from a series of 500ms alternating current pulses (ranging from −50 to 45 pA, 5pA increments) in current clamp mode and plotting the plateau voltage deflection against current amplitude. Rheobase and action potential (AP) properties were recorded using an ascending series of 10 ms depolarizing current pulses also in current clamp mode. Rheobase was defined as the lowest current to elicit a single AP. AP threshold was defined as the voltage when dV/dt first exceeded 28 mV/ms. AP amplitude was calculated relative to AP threshold, and AP half-width was measured at half of the AP amplitude.

Following current clamp recordings, voltage clamp was used to measure current responses to mechanical stimulation. DRG neuron membranes were mechanically displaced at 1.7 μm/V over 200 ms, 30 s intertrial interval, by a piezo stack actuator-driven borosilicate glass pipette (pipette velocity: 106.25 μm/ms). The first stimulation to elicit > 20pA of inward current was used to define mechanical threshold. Current density (pA/pF) was analyzed as a function of membrane indentation. Cells were only included in analysis if the leak current remained < 200 pA for all mechanical stimulations and if the patch was maintained for at least three membrane indentations. Current types were defined based on their inactivation time constants (τ) as 1) rapidly adapting (RA; $\tau < 10$ ms), 2) intermediately adapting (IA; 10 ms $\leq \tau \leq$ 30 ms), or 3) slowly adapting ($\tau > 30$ ms). If no significant differences in current type were observed, cells were broadly classified as mechanically sensitive (MS). Cells that never exhibited an inward current > 20pA in response to any mechanical stimulation were categorized as mechanically insensitive (MI).

2.6 Quantitative real time PCR

Townes AA (WT) and Townes SS (SCD) mice were anesthetized using isoflurane and decapitated, and lumbar 1-6 DRG and glabrous skin of the mouse hind paw were dissected. For hind paw tissue, the epidermis was separated from the underlying dermal layer, and only the epidermal layer was used for qRT-PCR. Tissue was manually homogenized in lysis buffer containing 1% 2-mercaptoethanol. RNA was isolated using a PureLink RNA Mini Kit (Invitrogen). RNA levels were standardized (5.12 ng/μL for DRG RNA, 7.2 ng/μL for keratinocyte RNA), and cDNA was synthesized using the SuperScript III First-Strand Synthesis System (Invitrogen). GAPDH was used as a loading control. qRT-PCR was run using a Bio-Rad CFX96 Touch Real-Time PCR Detection System, and fold gene expression was analyzed using the ΔΔCt method. Primers were obtained from Integrated DNA Technologies (Trpv4-F: TGCTTGTGTACCTGCTCTTC; Trpv4-R: CTCGTCACAGACCTTCATGTT; GAPDH-F: ACCACAGTCCATGCCATCAC; GAPDH-R: TCCACCACCCTGTTGCTGTA).

2.7. Statistical analysis

Data were analyzed using GraphPad Prism 9 or IBM SPSS Statistics 28.0. Since no sex differences were observed, data from both sexes were combined for analyses. For behavior experiments: von Frey up-down data and dry ice withdrawal latencies were analyzed using a two-way ANOVA; noxious needle and paintbrush response classifications were analyzed using Chi-square. For patch clamp experiments: membrane and AP properties were analyzed using a two-way ANOVA; mechanical current densities were analyzed using

a three-way mixed ANOVA; mechanical current thresholds were analyzed using a Kruskal-Wallis test; mechanical current types were analyzed using Chi-square. For calcium imaging experiments: proportion of cells responding data were analyzed using Chi-square, while response magnitude data were analyzed using two-way ANOVA. For qRT-PCR experiments, data were analyzed using unpaired Student's *t*-test. Results were considered statistically significant when $P < .05$; Bonferroni corrections were used for significant ANOVAs; Fisher's exact tests were used for significant Chi-square tests.

3. Results

3.1. Acute blockade of TRPV4 alleviates evoked hypersensitivity to punctate, but not dynamic, mechanical stimuli in SCD mice

We first examined the role of TRPV4 in SCD chronic mechanical allodynia. In comparison to WT mice, vehicle-injected SCD mice displayed pronounced mechanical hypersensitivity in the von Frey up-down assay (Fig. 1A). Among SCD mice, intraplantar injection of 300nM GSK2193874 significantly elevated von Frey withdrawal thresholds as compared to vehicle injection, effectively alleviating mechanical hypersensitivity (Fig. 1A).

Next, we investigated whether blocking TRPV4 with 300nM GSK2193874 in SCD mice would alleviate sensitivity to a noxious punctate mechanical stimulus by probing the hind paw with a spinal needle (Fig. 1B). WT controls demonstrated no change in the proportion of response type classification following TRPV4 inhibition with GSK2193874. However, compared to vehicle-treated SCD mice, SCD mice treated with 300nM GSK2193874 displayed significantly fewer nocifensive responses (Fig. 1B). This data suggests TRPV4 underlies sensitivity to noxious punctate mechanical stimulation in SCD.

Since SCD is characterized by sensitivity to light touch, including, for example, allodynia to increased wind speed[48], we further explored the role of TRPV4 in this form of mechanical allodynia in SCD using the dynamic light paintbrush assay (Fig 1C). Although vehicle-treated SCD mice demonstrated a non-significant reduction in the proportion of null responses relative to vehicle-treated WT controls, there was no change in response types for SCD mice when TRPV4 was blocked using 300nM GSK2193874 (Fig. 1C). Thus, sensitivity to light touch in SCD is not likely to be mediated by TRPV4.

Finally, since SCD patients commonly report heightened sensitivity to cold temperatures [15] and SCD mice display cold hypersensitivity[91,118], we examined the role of TRPV4 in cold hypersensitivity in SCD mice using dry ice stimulation of the hind paw (Fig. 1D). Vehicle-treated SCD mice displayed significant cold hypersensitivity relative to vehicle-treated WT controls, and TRPV4 block using 300nM GSK2193874 did not attenuate this effect. This is consistent with the evidence supporting a role for TRPV4 in heat sensation[36,99,115] rather than cold sensation. Overall, these behavioral data suggest that hypersensitivity to punctate, but not dynamic, mechanical stimulation in SCD is mediated by TRPV4, and that TRPV4 does not contribute to SCD cold hypersensitivity.

3.2. TRPV4 block reduces the proportion of mechanically sensitive small diameter DRG neurons from SCD mice

Our observation that TRPV4 blockade alleviates punctate mechanical hypersensitivity in SCD mice led us to ask whether this effect was mediated by dorsal root ganglia (DRG) neurons, which are essential for detecting and transducing somatosensory information to the central nervous system. Some evidence suggests that DRG neuron function depends on soma size[e.g., 66]. Larger diameter DRG neurons tend to give rise to myelinated Aβ and Aδ fibers, many, but not all, of which underlie innocuous mechanical sensation, while small DRG neurons are more likely to be unmyelinated C-fibers, and therefore are more likely to function as nociceptors[59]. Additionally, previous work from our lab indicates that small diameter DRG neurons from SCD mice display mechanical hypersensitivity using whole-cell patch clamp recordings of mechanically evoked inward currents[41]. We therefore used whole-cell patch clamp recordings of DRG neurons cultured from SCD mice or WT controls to determine whether blocking TRPV4 receptors with 300nM GSK2193874 would attenuate mechanical hypersensitivity in large (≥27μm) or small (<27μm) DRG neurons.

Whole-cell recordings were performed on cultured DRG neurons isolated from WT or SCD mice using either ENH recording solution or ENH containing 300nM of the TRPV4 inhibitor GSK2193874. Analysis of AP properties indicated that small diameter DRG neurons from SCD mice displayed significantly more hyperpolarized AP thresholds and larger AP amplitudes, regardless of treatment with GSK2193874 (Table 1). These changes in AP properties suggest that small DRG neurons from SCD mice display altered intrinsic excitability relative to WT, which is consistent with previous studies[66]. Analysis of mechanically evoked currents revealed a non-significant increase of inward current densities for small DRG neurons from SCD mice, an effect attenuated by TRPV4 blockade (Fig. 2A, B). Mechanical current thresholds were unaffected by genotype or treatment with the TRPV4 inhibitor (Fig. 2C). Current subtypes were not significantly affected by genotype or TRPV4 blockade, so currents were classified as either mechanically sensitive (MS; encompassing RA, IA, and SA currents) or mechanically insensitive (MI). TRPV4 block significantly increased the number of MI small DRG neurons from SCD mice but had no effect on the proportion of MI small DRG neurons from WT controls (Fig. 2D). These data suggest that TRPV4 blockade effectively reduces the mechanical sensitivity of small DRG neurons from SCD mice.

Whole-cell patch clamp recordings of large diameter DRG neurons revealed that blocking TRPV4 with 300nM GSK2193874 significantly depolarized RMP and reduced rheobase values overall, and among DRG neurons from SCD mice, GSK2193874 significantly reduced rheobase relative to neurons recorded in ENH alone (Table 2). This suggests that blocking TRPV4 receptors of large DRG neurons may alter intrinsic excitability. Mechanical stimulation of large DRG neurons revealed a modest and non-significant reduction of inward current density for both WT and SCD groups following TRPV4 block (Supplemental Fig. 1A, B), and unchanged mechanical thresholds (Supplemental Fig. 1C). Combination of RA, IA, and SA currents broadly as mechanically sensitive (MS) revealed that most recorded neurons displayed some form of mechanical sensitivity, and there were no genotype or TRPV4-mediated effects on this simplified classification (Supplemental Fig. 1D). Together,

these data suggest that TRPV4 antagonist-mediated reductions in somatic mechanical sensitivity in SCD occur selectively in small DRG neurons.

3.3. TRPV4-mediated calcium flux is sensitized in small diameter DRG neurons from SCD mice

To further examine the cellular mechanisms of TRPV4-mediated hypersensitivity in SCD, we performed calcium imaging of DRG neurons isolated from WT or SCD mice in the presence of 30nM, 100nM, 300nM, or 1000nM of GSK1016790A, a TRPV4-selective agonist (Fig. 3A, B). Like our patch clamp experiments, data from small and large diameter DRG neurons were analyzed separately. For small DRG neurons, although we observed no effect of genotype on the percentage of neurons that responded to the TRPV4 agonist (Fig. 3C), application of 100nM GSK1016790A evoked significantly larger calcium responses in neurons from SCD mice relative to WT (Fig. 3D), suggesting that small DRG neurons from SCD mice display selective sensitization when TRPV4 is pharmacologically activated using specific concentrations of the agonist. Analysis of baseline calcium responses for small DRG neurons indicated no significant differences between WT and SCD neurons ($t_{(493)}$ = 1.157, p = .248).

We also performed calcium imaging of large DRG neurons isolated from SCD mice or WT controls, using 30nM, 100nM, 300nM, or 1000nM of the TRPV4 agonist GSK1016790A (Supplemental Fig. 2A, B). Although significantly more large diameter DRG neurons from SCD mice responded to 300nM GSK1016790A (Supplemental Fig. 2C), response magnitudes of DRG neurons from SCD mice were significantly reduced relative to WT controls (Supplemental Fig. 2D). This suggests that TRPV4 receptors are likely not sensitized in large diameter DRG neurons from SCD mice. Additionally, analysis of baseline calcium responses for large DRG neurons indicated no significant differences between WT and SCD neurons ($t_{(137)}$ = 1.535, p = .127). Together, these data indicate that TRPV4 induced calcium responses are sensitized in small, not large, DRG neurons from SCD mice relative to WT.

3.4. Keratinocytes isolated from SCD mice display sensitized calcium responses when TRPV4 is activated

Keratinocytes constitute the majority of cells within the epidermis[30,32], are located near sensory nerve terminals[1,56,63,74], and are involved in TRPV4-mediated hypersensitivity following injury[72]. Thus, TRPV4 activity in these cells may also contribute to SCD hypersensitivity. To determine whether TRPV4 is sensitized in keratinocytes from SCD mice, we measured calcium responses in primary keratinocyte cultures from WT (Fig. 4A) and SCD mice (Fig. 4B) during application of the TRPV4 agonist GSK1016790A. Keratinocytes were isolated from SCD mice and WT controls, and exposed to 1nM, 3nM, 6nM, or 10nM GSK1016790A. Significantly more keratinocytes from SCD mice responded to application of 3, 6, and 10nM GSK1016790A relative to keratinocytes from WT mice (Fig. 4C), and the magnitude of TRPV4-induced (6nM GSK1016790A) calcium flux in keratinocytes from SCD mice was significantly increased relative to that observed in WT cells (Fig. 4D). Although analysis of baseline calcium responses indicated a significant increase for SCD keratinocytes relative to WT ($t_{(1132)}$ = 3.98, p < .0001), there was

not a significant relationship between baseline and 6nM GSK1016790A-induced calcium responses for SCD keratinocytes (Pearson's $r = -0.103$, $p = .117$), suggesting baseline SCD keratinocyte calcium responses do not predict TRPV4 agonist-induced responses. These data suggest that TRPV4 is sensitized in keratinocytes from SCD mice, and thus these cells likely contribute to the behavioral hypersensitivity observed in SCD mice (Fig. 1).

3.5. No change in TRPV4 mRNA expression in SCD DRG neurons or keratinocytes

To determine whether the behavioral and functional TRPV4-mediated sensitization observed in SCD is due to altered TRPV4 expression, qRT-PCR was performed on DRG and keratinocyte tissue isolated from WT and SCD mice. Analysis of TRPV4 mRNA indicated no expression differences between WT and SCD mice, either at the level of the DRG or keratinocyte (Supplemental Fig. 3). Although there is a trend for reduced TRPV4 mRNA expression in DRG neurons, this would not explain the TRPV4-mediated sensitization we observed in small DRG neurons. Thus, these data suggest that the TRPV4 antagonist-induced reversal of mechanical hyperalgesia observed in SCD mice is likely due to sensitized function as opposed to altered expression, of TRPV4.

4. Discussion

The current study is the first to demonstrate a role for TRPV4 in the chronic mechanical hypersensitivity prevalent in SCD. SCD mice display punctate mechanical hypersensitivity that is attenuated by TRPV4 blockade. Small diameter DRG neurons from SCD mice demonstrate sensitized TRPV4-mediated calcium responses and increased mechanical sensitivity that is mitigated by TRPV4 receptor blockade. Finally, we demonstrate for the first time that epidermal keratinocytes from SCD mice are sensitized relative to controls; SCD keratinocytes exhibit robust increases of TRPV4-mediated calcium responses relative to keratinocytes from WT mice. Together these data indicate that TRPV4 activity in numerous peripheral cell types contributes to the mechanical allodynia prevalent in SCD.

4.1. TRPV4 block attenuates mechanical hypersensitivity to punctate, not dynamic, mechanical stimuli

Our finding that SCD mice display hypersensitivity to mechanical and cold stimuli is consistent with previous findings from our lab[33,41,87,91,118,119] and others[18,20,39,40,51,53,54,60,61,66,84,114]. Given other evidence implicating TRPV4 in various pain models, including those of an inflammatory [4,5,9,22–24,99,121,122] and neuropathic nature [6,7,67,68,120], we expected TRPV4 to also be involved in SCD pain given that SCD pain has both inflammatory and neuropathic attributes[3]. Indeed, acutely blocking TRPV4 receptors alleviated von Frey and noxious needle mechanical allodynia, indicating this channel contributes to mechanical hypersensitivity in this model. We did not observe a similar effect of TRPV4 bock on hypersensitivity to dynamic light touch. This could reflect a differential role for TRPV4 in mediating responses to mechanical stimuli that are of distinct valences and detected by separate fiber types. A-fibers (e.g., low-threshold mechanoreceptor (LTMR) Aβ) and C LTMRs likely mediate dynamic light touch with a brush for example [44,52,57,73,79], whereas punctate or pressure stimuli are associated several types of sensory fibers and transduction mechanisms, including A-fibers, C-fibers,

under inflammatory conditions [55,58]. Indeed, the majority of DRG neurons that express TRPV4 are small diameter nociceptors[103,104], which tend to give rise to unmyelinated C-fibers or lightly myelinated Aδ-fibers[28,93]. It is also possible that in SCD mice TRPV4 is selectively expressed in subpopulations of DRG neurons known to support allodynia to punctate but not light touch stimuli, including CGRPα-positive neurons [26]. Thus, future studies will need to determine whether this selective attenuation of hypersensitivity to punctate, but not dynamic, mechanical stimuli is due to differential function or TRPV4 expression in these fiber types.

Although other TRP channels, including TRPM8, TRPA1, and TRPC5, are known to mediate cold sensation[17,62], there is a lack of evidence for TRPV4 in cold sensation. Consistent with this, we found that SCD mice demonstrated significant cold hypersensitivity, an effect that was not reversed by acute TRPV4 block. Thus, the potential therapeutic value of a TRPV4 inhibitor in SCD is likely limited to that of mechanical hypersensitivity, and alleviation of cold-triggered pain in patients with SCD[12,45,82] will likely need to be supported by another mechanism.

Consistent with previous work from our lab[87], paintbrush stimulation evoked some nocifensive-like behaviors in WT mice (Fig. 1C), suggesting a possible role for C-fiber nociceptors in this response. Interestingly, previous research suggests C-fibers are capable of multimodal responses where aversive behaviors are elicited by fast ionotropic stimulation of C-fiber afferents, while itch responses are observed following metabotropic C-fiber stimulation[96]. Therefore, the observed aversive responses in WT mice in the present study may stem from brush-induced ionotropic activation of nociceptors, although additional experiments are needed to address this possibility.

4.2 Small diameter DRG neurons preferentially drive TRPV4-mediated sensitization in SCD

Building on previous studies showing mechanical allodynia in SCD is associated with sensitized DRG neuron activity[41,43,66,91], we examined how TRPV4 might be involved in SCD pain by performing whole-cell patch clamp recordings and calcium imaging of DRG neurons. Our findings suggest TRPV4-mediated sensitization occurs at the level of small, but not large, DRG neurons. This is consistent with previous research in rodents indicating small DRG neurons give rise to putative unmyelinated C-fiber nociceptors[28,31,59], and with other findings demonstrating that TRPV4 is more highly expressed in small diameter mouse DRG neurons than large [103,104].

Our patch clamp recordings indicate TRPV4 blockade increases the number of small DRG neurons from SCD mice that are insensitive to mechanical stimulation, which is consistent with previous findings that blocking other TRP channels (i.e., TRPV1, TRPC5) reduced the proportion of small DRG neurons from SCD mice that responded to mechanical stimuli[41,89]. Indeed, others have found a selective role for smaller dissociated DRG neurons in SCD hypersensitivity using targeted approaches. For instance, small and medium diameter DRG neurons from SCD mice displayed increased intrinsic excitability, while large diameter DRG neurons from SCD mice demonstrated no change from large DRG control neurons, which was accompanied by increased Nav1.8 current density in small neurons[66].

Taken together with our current findings, TRPV4 is likely driving SCD hypersensitivity at the level of the small diameter DRG neuron.

4.3 Keratinocytes as a novel cell type in SCD hypersensitivity

Keratinocytes are the first point of contact we have with our external environment. They are proximal to sensory nerve terminals[1,56,63,74], make synapse-like connections with these terminals[107], are involved in peripheral somatosensation[70,71], and mediate peripheral neuron activity[14,70]. As such, they are well-suited to be involved in hypersensitivity in SCD, and in fact, our calcium imaging data suggest they may play a role in TRPV4-mediated SCD hypersensitivity. Indeed, skin keratinocytes highly express TRPV4 protein[23,25,36,100,104], and epidermal TRPV4 is involved in UV light-induced nocifensive behaviors[72]. Thus, our data are consistent with a role for TRPV4 in peripheral SCD hypersensitivity at the level of the keratinocyte, and for the first time suggest that epidermal keratinocytes may play a role in persistent SCD pain.

4.4 Possible mechanisms underlying TRPV4-mediated sensitization in SCD

Several endogenous factors that are aberrant in SCD may be sensitizing TRPV4 receptors in peripheral neurons and keratinocytes, including endothelin-1 (ET-1) [66], arachidonic acid[2,116], or tryptase-induced activation of protease-activated receptor 2 (PAR2), stemming from mast cell degranulation[111,114]. Primarily acting on endothelin type A (ET_A) receptors[81], ET-1 is a peptide that is elevated at baseline and further increased during a VOC in plasma from patients with SCD[35,86]. Additionally, DRG neurons from SCD mice display elevated ET-1 and ET_A expression[66]. In SCD mice, when ET_A receptors are knocked down, hypersensitivity to mechanical and thermal stimuli is reduced, and elevated Nav1.8 currents are reduced when ET_A receptors are blocked[66]. In keratinocytes, endothelin signaling may depend on TRPV4 function in a UV light model of sunburn pain, as ET-1-mediated sensitization of UV light-induced calcium flux in keratinocytes is suppressed when TRPV4 receptors are blocked[72]. Interestingly, ET-1 and ET_A receptor expression in hind paw skin is similar between SCD mice and controls[66], and further work is needed to determine whether this differential expression affects SCD keratinocyte function. TRPV4-mediated sensitization in SCD keratinocytes may also be due to additional mechanisms, for example, altered arachidonic acid levels [2] or PAR2 signaling[111,122], or perhaps by interactions with bona fide mechanotransducers (e.g., PIEZO1)[69,95,105,106,117]. Therefore, future work will be needed to determine whether keratinocyte hypersensitivity in SCD is mediated by these, or other pathways.

There are several lines of evidence that suggest TRPV4 mediates mechanical hyperalgesia in neuropathic injury models, including diabetes and chemotherapy-induced peripheral neuropathy[6], and inflammatory pain models[5,99], but not normal (non-injury) mechanical sensation. In fact, naïve TRPV4 knockout mice display normal behavioral responses to mechanical stimulation[103]. Additional evidence suggests TRPV4 currents are not increased by mechanical displacement of the membrane[64,102,103]. Thus, TRPV4 is likely to mediate the mechanical hypersensitivity associated with neuropathy or inflammation, but not normal mechanotransduction. The current study suggests TRPV4 function in small diameter DRG neurons is altered in the SCD model of pain, while TRPV4 function in large

diameter DRG neurons from SCD mice remains unchanged. One possible explanation is that TRPV4 expression levels may differ between small and large diameter DRG neurons from SCD mice, or that distinct mechanisms contribute to TRPV4 sensitization in these different DRG neuron populations. Future work will be necessary to explore these possibilities.

These results provide new insight into the role of TRPV4 ion channels in SCD pathophysiology, paving the way for potential novel therapeutics in the treatment of SCD chronic pain. While the current study used only one TRPV4 agonist (GSK1016790A) and one TRPV4 antagonist (GSK2193874), these were chosen for their high degree of specificity and potency[27,109,110]. Although we investigated the effect of several different concentrations of these drugs in our experiments, one limitation of the currently study is that other pharmacological manipulations of TRPV4 activity were not employed. Additionally, we acknowledge that the GSKS1016790A-induced sensitization of calcium flux in SCD keratinocytes may reflect sensitization of TRPV4 channels, or it may be due to broader cellular impairment of intracellular calcium buffering, however, additional experiments are needed to address this. Furthermore, although there is a small but significant elevation of baseline calcium responses in keratinocytes from SCD mice relative to WT, there is no significant relationship between baseline calcium responses and those evoked by 6nM of the TRPV4 agonist in SCD keratinocytes. Ultimately this suggests the TRPV4 agonist-induced increase of calcium responses in SCD keratinocytes are not caused by underlying impairment of calcium buffering, but instead are due to TRPV4 channel sensitization in SCD.

Chronic SCD pain is linked to an enormous healthcare burden[13], and current pain treatments, which include NSAIDS[37,80] and opioids[3], are primarily used to treat acute pain episodes and are inadequate for managing chronic pain. Further, additional barriers to treatment prevent patients with SCD from receiving much needed opioid therapeutics during pain crises due to discrimination by select healthcare professionals in emergency departments[34,38]. Thus, there is a pressing need to facilitate more effective pain management strategies to ease the pain burden for those patients living with persistent SCD pain.

Supplementary Material

Refer to Web version on PubMed Central for supplementary material.

Acknowledgements

The authors thank Anthony Menzel and Christina Mecca for technical assistance.

Funding:

This research was supported by NIH grants NS070711 (to C.L.S), NS108278 (to C.L.S), HL155791 (to K.E.S.), and NS124833 (to V.L.E.).

References

[1]. Abraira VE, Ginty DD. The sensory neurons of touch. Neuron 2013;79(4):618–639. [PubMed: 23972592]

[2]. Adebiyi MG, Manalo JM, Xia Y. Metabolomic and molecular insights into sickle cell disease and innovative therapies. Blood Adv 2019;3(8):1347–1355. [PubMed: 31015210]

[3]. Aich A, Jones MK, Gupta K. Pain and sickle cell disease. Curr Opin Hematol 2019;26(3):131–138. [PubMed: 30893088]

[4]. Alessandri-Haber N, Dina OA, Chen X, Levine JD. TRPC1 and TRPC6 channels cooperate with TRPV4 to mediate mechanical hyperalgesia and nociceptor sensitization. J Neurosci 2009;29(19):6217–6228. [PubMed: 19439599]

[5]. Alessandri-Haber N, Dina OA, Joseph EK, Reichling D, Levine JD. A transient receptor potential vanilloid 4-dependent mechanism of hyperalgesia is engaged by concerted action of inflammatory mediators. J Neurosci 2006;26(14):3864–3874. [PubMed: 16597741]

[6]. Alessandri-Haber N, Dina OA, Joseph EK, Reichling DB, Levine JD. Interaction of transient receptor potential vanilloid 4, integrin, and SRC tyrosine kinase in mechanical hyperalgesia. J Neurosci 2008;28(5):1046–1057. [PubMed: 18234883]

[7]. Alessandri-Haber N, Dina OA, Yeh JJ, Parada CA, Reichling DB, Levine JD. Transient receptor potential vanilloid 4 is essential in chemotherapy-induced neuropathic pain in the rat. J Neurosci 2004;24(18):4444–4452. [PubMed: 15128858]

[8]. Alessandri-Haber N, Joseph E, Dina OA, Liedtke W, Levine JD. TRPV4 mediates pain-related behavior induced by mild hypertonic stimuli in the presence of inflammatory mediator. Pain 2005;118(1–2):70–79. [PubMed: 16213085]

[9]. Alessandri-Haber N, Yeh JJ, Boyd AE, Parada CA, Chen X, Reichling DB, Levine JD. Hypotonicity induces TRPV4-mediated nociception in rat. Neuron 2003;39(3):497–511. [PubMed: 12895423]

[10]. Alexander R, Kerby A, Aubdool AA, Power AR, Grover S, Gentry C, Grant AD. 4alpha-phorbol 12,13-didecanoate activates cultured mouse dorsal root ganglia neurons independently of TRPV4. Br J Pharmacol 2013;168(3):761–772. [PubMed: 22928864]

[11]. Almeida LEF, Damsker JM, Albani S, Afsar N, Kamimura S, Pratt D, Kleiner DE, Quezado M, Gordish-Dressman H, Quezado ZMN. The corticosteroid compounds prednisolone and vamorolone do not alter the nociception phenotype and exacerbate liver injury in sickle cell mice. Sci Rep 2018;8(1):6081. [PubMed: 29666400]

[12]. Amjad H, Bannerman RM, Judisch JM. Letter: Sickling pain and season. Br Med J 1974;2(5909):54.

[13]. Baldwin Z, Jiao B, Basu A, Roth J, Bender MA, Elsisi Z, Johnson KM, Cousin E, Ramsey SD, Devine B. Medical and Non-medical Costs of Sickle Cell Disease and Treatments from a US Perspective: A Systematic Review and Landscape Analysis. Pharmacoecon Open 2022;6(4):469–481. [PubMed: 35471578]

[14]. Baumbauer KM, DeBerry JJ, Adelman PC, Miller RH, Hachisuka J, Lee KH, Ross SE, Koerber HR, Davis BM, Albers KM. Keratinocytes can modulate and directly initiate nociceptive responses. Elife 2015;4.

[15]. Brandow AM, Stucky CL, Hillery CA, Hoffmann RG, Panepinto JA. Patients with sickle cell disease have increased sensitivity to cold and heat. Am J Hematol 2013;88(1):37–43. [PubMed: 23115062]

[16]. Brenner DS, Golden JP, Gereau RWt. A novel behavioral assay for measuring cold sensation in mice. PLoS One 2012;7(6):e39765. [PubMed: 22745825]

[17]. Buijs TJ, McNaughton PA. The Role of Cold-Sensitive Ion Channels in Peripheral Thermosensation. Front Cell Neurosci 2020;14:262. [PubMed: 32973456]

[18]. Cain DM, Vang D, Simone DA, Hebbel RP, Gupta K. Mouse models for studying pain in sickle disease: effects of strain, age, and acuteness. Br J Haematol 2012;156(4):535–544. [PubMed: 22171826]

[19]. Cataldo G, Lunzer MM, Olson JK, Akgun E, Belcher JD, Vercellotti GM, Portoghese PS, Simone DA. Bivalent ligand MCC22 potently attenuates nociception in a murine model of sickle cell disease. Pain 2018;159(7):1382–1391. [PubMed: 29578946]

[20]. Cataldo G, Rajput S, Gupta K, Simone DA. Sensitization of nociceptive spinal neurons contributes to pain in a transgenic model of sickle cell disease. Pain 2015;156(4):722–730. [PubMed: 25630029]

[21]. Chaplan SR, Bach FW, Pogrel JW, Chung JM, Yaksh TL. Quantitative assessment of tactile allodynia in the rat paw. J Neurosci Methods 1994;53(1):55–63. [PubMed: 7990513]

[22]. Chen X, Alessandri-Haber N, Levine JD. Marked attenuation of inflammatory mediator-induced C-fiber sensitization for mechanical and hypotonic stimuli in TRPV4-/- mice. Mol Pain 2007;3:31. [PubMed: 17967183]

[23]. Chen Y, Kanju P, Fang Q, Lee SH, Parekh PK, Lee W, Moore C, Brenner D, Gereau RWt, Wang F, Liedtke W. TRPV4 is necessary for trigeminal irritant pain and functions as a cellular formalin receptor. Pain 2014;155(12):2662–2672. [PubMed: 25281928]

[24]. Chen Y, Williams SH, McNulty AL, Hong JH, Lee SH, Rothfusz NE, Parekh PK, Moore C, Gereau RWt, Taylor AB, Wang F, Guilak F, Liedtke W. Temporomandibular joint pain: a critical role for Trpv4 in the trigeminal ganglion. Pain 2013;154(8):1295–1304. [PubMed: 23726674]

[25]. Chung MK, Lee H, Mizuno A, Suzuki M, Caterina MJ. TRPV3 and TRPV4 mediate warmth-evoked currents in primary mouse keratinocytes. J Biol Chem 2004;279(20):21569–21575. [PubMed: 15004014]

[26]. Cowie AM, Moehring F, O'Hara C, Stucky CL. Optogenetic Inhibition of CGRPalpha Sensory Neurons Reveals Their Distinct Roles in Neuropathic and Incisional Pain. J Neurosci 2018;38(25):5807–5825. [PubMed: 29925650]

[27]. Darby WG, Grace MS, Baratchi S, McIntyre P. Modulation of TRPV4 by diverse mechanisms. Int J Biochem Cell Biol 2016;78:217–228. [PubMed: 27425399]

[28]. Devor M Unexplained peculiarities of the dorsal root ganglion. Pain 1999;Suppl 6:S27–S35. [PubMed: 10491970]

[29]. Dixon WJ. The Up-and-Down Method for Small Samples. Journal of the American Statistical Association 1965;60(312):967–978.

[30]. Eckert RL, Rorke EA. Molecular biology of keratinocyte differentiation. Environ Health Perspect 1989;80:109–116. [PubMed: 2466639]

[31]. Esposito MF, Malayil R, Hanes M, Deer T. Unique Characteristics of the Dorsal Root Ganglion as a Target for Neuromodulation. Pain Med 2019;20(Suppl 1):S23–S30.

[32]. Fuchs E Keratins and the skin. Annu Rev Cell Dev Biol 1995;11:123–153. [PubMed: 8689554]

[33]. Garrison SR, Kramer AA, Gerges NZ, Hillery CA, Stucky CL. Sickle cell mice exhibit mechanical allodynia and enhanced responsiveness in light touch cutaneous mechanoreceptors. Mol Pain 2012;8:62. [PubMed: 22963123]

[34]. Glassberg J, Tanabe P, Richardson L, Debaun M. Among emergency physicians, use of the term "Sickler" is associated with negative attitudes toward people with sickle cell disease. Am J Hematol 2013;88(6):532–533. [PubMed: 23526459]

[35]. Graido-Gonzalez E, Doherty JC, Bergreen EW, Organ G, Telfer M, McMillen MA. Plasma endothelin-1, cytokine, and prostaglandin E2 levels in sickle cell disease and acute vaso-occlusive sickle crisis. Blood 1998;92(7):2551–2555. [PubMed: 9746797]

[36]. Guler AD, Lee H, Iida T, Shimizu I, Tominaga M, Caterina M. Heat-evoked activation of the ion channel, TRPV4. J Neurosci 2002;22(15):6408–6414. [PubMed: 12151520]

[37]. Han J, Saraf SL, Lash JP, Gordeuk VR. Use of anti-inflammatory analgesics in sickle-cell disease. J Clin Pharm Ther 2017;42(5):656–660. [PubMed: 28695614]

[38]. Haywood C Jr., Tanabe P, Naik R, Beach MC, Lanzkron S. The impact of race and disease on sickle cell patient wait times in the emergency department. Am J Emerg Med 2013;31(4):651–656. [PubMed: 23380119]

[39]. He Y, Chen Y, Tian X, Yang C, Lu J, Xiao C, DeSimone J, Wilkie DJ, Molokie RE, Wang ZJ. CaMKIIalpha underlies spontaneous and evoked pain behaviors in Berkeley sickle cell transgenic mice. Pain 2016;157(12):2798–2806. [PubMed: 27842048]

[40]. He Y, Wilkie DJ, Nazari J, Wang R, Messing RO, DeSimone J, Molokie RE, Wang ZJ. PKCdelta-targeted intervention relieves chronic pain in a murine sickle cell disease model. J Clin Invest 2016;126(8):3053–3057. [PubMed: 27348590]

[41]. Hillery CA, Kerstein PC, Vilceanu D, Barabas ME, Retherford D, Brandow AM, Wandersee NJ, Stucky CL. Transient receptor potential vanilloid 1 mediates pain in mice with severe sickle cell disease. Blood 2011;118(12):3376–3383. [PubMed: 21708890]

[42]. Hogan Q, Sapunar D, Modric-Jednacak K, McCallum JB. Detection of neuropathic pain in a rat model of peripheral nerve injury. Anesthesiology 2004;101(2):476–487. [PubMed: 15277932]

[43]. Hu X, Adebiyi MG, Luo J, Sun K, Le TT, Zhang Y, Wu H, Zhao S, Karmouty-Quintana H, Liu H, Huang A, Wen YE, Zaika OL, Mamenko M, Pochynyuk OM, Kellems RE, Eltzschig HK, Blackburn MR, Walters ET, Huang D, Hu H, Xia Y. Sustained Elevated Adenosine via ADORA2B Promotes Chronic Pain through Neuro-immune Interaction. Cell Rep 2016;16(1):106–119. [PubMed: 27320922]

[44]. Huzard D, Martin M, Maingret F, Chemin J, Jeanneteau F, Mery PF, Fossat P, Bourinet E, Francois A. The impact of C-tactile low-threshold mechanoreceptors on affective touch and social interactions in mice. Sci Adv 2022;8(26):eabo7566. [PubMed: 35767616]

[45]. Ibrahim AS. Relationship between meteorological changes and occurrence of painful sickle cell crises in Kuwait. Trans R Soc Trop Med Hyg 1980;74(2):159–161. [PubMed: 7385294]

[46]. Ingram VM. A specific chemical difference between the globins of normal human and sickle-cell anaemia haemoglobin. Nature 1956;178(4537):792–794. [PubMed: 13369537]

[47]. Jacob E, Chan VW, Hodge C, Zeltzer L, Zurakowski D, Sethna NF. Sensory and Thermal Quantitative Testing in Children With Sickle Cell Disease. J Pediatr Hematol Oncol 2015;37(3):185–189. [PubMed: 25014619]

[48]. Jones S, Duncan ER, Thomas N, Walters J, Dick MC, Height SE, Stephens AD, Thein SL, Rees DC. Windy weather and low humidity are associated with an increased number of hospital admissions for acute pain and sickle cell disease in an urban environment with a maritime temperate climate. Br J Haematol 2005;131(4):530–533. [PubMed: 16281945]

[49]. Kenyon N, Wang L, Spornick N, Khaibullina A, Almeida LE, Cheng Y, Wang J, Guptill V, Finkel JC, Quezado ZM. Sickle cell disease in mice is associated with sensitization of sensory nerve fibers. Exp Biol Med (Maywood) 2015;240(1):87–98. [PubMed: 25070860]

[50]. Khaibullina A, Almeida LE, Wang L, Kamimura S, Wong EC, Nouraie M, Maric I, Albani S, Finkel J, Quezado ZM. Rapamycin increases fetal hemoglobin and ameliorates the nociception phenotype in sickle cell mice. Blood Cells Mol Dis 2015;55(4):363–372. [PubMed: 26460261]

[51]. Khasabova IA, Uhelski M, Khasabov SG, Gupta K, Seybold VS, Simone DA. Sensitization of nociceptors by prostaglandin E2-glycerol contributes to hyperalgesia in mice with sickle cell disease. Blood 2019;133(18):1989–1998. [PubMed: 30796025]

[52]. Kilo S, Schmelz M, Koltzenburg M, Handwerker HO. Different patterns of hyperalgesia induced by experimental inflammation in human skin. Brain 1994;117 (Pt 2):385–396. [PubMed: 8186964]

[53]. Kiven S, Wang Y, Aich A, Argueta DA, Lei J, Sagi V, Tennakoon M, Bedros SJ, Lambrecht N, Gupta K. Spatiotemporal Alterations in Gait in Humanized Transgenic Sickle Mice. Front Immunol 2020;11:561947. [PubMed: 33178189]

[54]. Kohli DR, Li Y, Khasabov SG, Gupta P, Kehl LJ, Ericson ME, Nguyen J, Gupta V, Hebbel RP, Simone DA, Gupta K. Pain-related behaviors and neurochemical alterations in mice expressing sickle hemoglobin: modulation by cannabinoids. Blood 2010;116(3):456–465. [PubMed: 20304807]

[55]. Koltzenburg M, Lundberg LER, Torebjork EH. Dynamic and static components of mechanical hyperalgesia in human hairy skin. Pain 1992;51(2):207–219. [PubMed: 1484717]

[56]. Kruger L, Perl ER, Sedivec MJ. Fine structure of myelinated mechanical nociceptor endings in cat hairy skin. J Comp Neurol 1981;198(1):137–154. [PubMed: 7229137]

[57]. Kumazawa T, Perl ER. Primate cutaneous sensory units with unmyelinated (C) afferent fibers. J Neurophysiol 1977;40(6):1325–1338. [PubMed: 411895]

[58]. La JH, Chung JM. Peripheral afferents and spinal inhibitory system in dynamic and static mechanical allodynia. Pain 2017;158(12):2285–2289. [PubMed: 28885453]

[59]. Le Pichon CE, Chesler AT. The functional and anatomical dissection of somatosensory subpopulations using mouse genetics. Front Neuroanat 2014;8:21. [PubMed: 24795573]

[60]. Lei J, Benson B, Tran H, Ofori-Acquah SF, Gupta K. Comparative Analysis of Pain Behaviours in Humanized Mouse Models of Sickle Cell Anemia. PLoS One 2016;11(8):e0160608. [PubMed: 27494522]

[61]. Lei J, Paul J, Wang Y, Gupta M, Vang D, Thompson S, Jha R, Nguyen J, Valverde Y, Lamarre Y, Jones MK, Gupta K. Heme Causes Pain in Sickle Mice via Toll-Like Receptor 4-Mediated Reactive Oxygen Species- and Endoplasmic Reticulum Stress-Induced Glial Activation. Antioxid Redox Signal 2021;34(4):279–293. [PubMed: 32729340]

[62]. Lezama-Garcia K, Mota-Rojas D, Pereira AMF, Martinez-Burnes J, Ghezzi M, Dominguez A, Gomez J, de Mira Geraldo A, Lendez P, Hernandez-Avalos I, Falcon I, Olmos-Hernandez A, Wang D. Transient Receptor Potential (TRP) and Thermoregulation in Animals: Structural Biology and Neurophysiological Aspects. Animals (Basel) 2022;12(1).

[63]. Li L, Ginty DD. The structure and organization of lanceolate mechanosensory complexes at mouse hair follicles. Elife 2014;3:e01901. [PubMed: 24569481]

[64]. Liedtke W, Choe Y, Marti-Renom MA, Bell AM, Denis CS, Sali A, Hudspeth AJ, Friedman JM, Heller S. Vanilloid receptor-related osmotically activated channel (VR-OAC), a candidate vertebrate osmoreceptor. Cell 2000;103(3):525–535. [PubMed: 11081638]

[65]. Liu TT, Bi HS, Lv SY, Wang XR, Yue SW. Inhibition of the expression and function of TRPV4 by RNA interference in dorsal root ganglion. Neurol Res 2010;32(5):466–471. [PubMed: 19278577]

[66]. Lutz BM, Wu S, Gu X, Atianjoh FE, Li Z, Fox BM, Pollock DM, Tao YX. Endothelin type A receptors mediate pain in a mouse model of sickle cell disease. Haematologica 2018;103(7):1124–1135. [PubMed: 29545351]

[67]. Materazzi S, Fusi C, Benemei S, Pedretti P, Patacchini R, Nilius B, Prenen J, Creminon C, Geppetti P, Nassini R. TRPA1 and TRPV4 mediate paclitaxel-induced peripheral neuropathy in mice via a glutathione-sensitive mechanism. Pflugers Arch 2012;463(4):561–569. [PubMed: 22258694]

[68]. Matsumura Y, Yokoyama Y, Hirakawa H, Shigeto T, Futagami M, Mizunuma H. The prophylactic effects of a traditional Japanese medicine, goshajinkigan, on paclitaxel-induced peripheral neuropathy and its mechanism of action. Mol Pain 2014;10:61. [PubMed: 25240613]

[69]. Miyamoto T, Mochizuki T, Nakagomi H, Kira S, Watanabe M, Takayama Y, Suzuki Y, Koizumi S, Takeda M, Tominaga M. Functional role for Piezo1 in stretch-evoked Ca(2)(+) influx and ATP release in urothelial cell cultures. J Biol Chem 2014;289(23):16565–16575. [PubMed: 24759099]

[70]. Moehring F, Cowie AM, Menzel AD, Weyer AD, Grzybowski M, Arzua T, Geurts AM, Palygin O, Stucky CL. Keratinocytes mediate innocuous and noxious touch via ATP-P2X4 signaling. Elife 2018;7.

[71]. Moehring F, Mikesell AR, Sadler KE, Menzel AD, Stucky CL. Piezo1 Mediates Keratinocyte Mechanotransduction. bioRxiv 2020:2020.2007.2019.211086.

[72]. Moore C, Cevikbas F, Pasolli HA, Chen Y, Kong W, Kempkes C, Parekh P, Lee SH, Kontchou NA, Yeh I, Jokerst NM, Fuchs E, Steinhoff M, Liedtke WB. UVB radiation generates sunburn pain and affects skin by activating epidermal TRPV4 ion channels and triggering endothelin-1 signaling. Proc Natl Acad Sci U S A 2013;110(34):E3225–3234. [PubMed: 23929777]

[73]. Olausson H, Lamarre Y, Backlund H, Morin C, Wallin BG, Starck G, Ekholm S, Strigo I, Worsley K, Vallbo AB, Bushnell MC. Unmyelinated tactile afferents signal touch and project to insular cortex. Nat Neurosci 2002;5(9):900–904. [PubMed: 12145636]

[74]. Owens DM, Lumpkin EA. Diversification and specialization of touch receptors in skin. Cold Spring Harb Perspect Med 2014;4(6).

[75]. Pang Z, Sakamoto T, Tiwari V, Kim YS, Yang F, Dong X, Guler AD, Guan Y, Caterina MJ. Selective keratinocyte stimulation is sufficient to evoke nociception in mice. Pain 2015;156(4):656–665. [PubMed: 25790456]

[76]. Paszty C, Brion CM, Manci E, Witkowska HE, Stevens ME, Mohandas N, Rubin EM. Transgenic knockout mice with exclusively human sickle hemoglobin and sickle cell disease. Science 1997;278(5339):876–878. [PubMed: 9346488]

[77]. Paul JA, Aich A, Abrahante JE, Wang Y, LaRue RS, Rathe SK, Kalland K, Mittal A, Jha R, Peng F, Largaespada DA, Bagchi A, Gupta K. Transcriptomic analysis of gene signatures associated with sickle pain. Sci Data 2017;4:170051. [PubMed: 29292796]

[78]. Pauling L, Itano HA, et al. Sickle cell anemia a molecular disease. Science 1949;110(2865):543–548. [PubMed: 15395398]

[79]. Perini I, Olausson H, Morrison I. Seeking pleasant touch: neural correlates of behavioral preferences for skin stroking. Front Behav Neurosci 2015;9:8. [PubMed: 25698948]

[80]. Perlin E, Finke H, Castro O, Rana S, Pittman J, Burt R, Ruff C, McHugh D. Enhancement of pain control with ketorolac tromethamine in patients with sickle cell vaso-occlusive crisis. Am J Hematol 1994;46(1):43–47. [PubMed: 7514356]

[81]. Pomonis JD, Rogers SD, Peters CM, Ghilardi JR, Mantyh PW. Expression and localization of endothelin receptors: implications for the involvement of peripheral glia in nociception. J Neurosci 2001;21(3):999–1006. [PubMed: 11157085]

[82]. Redwood AM, Williams EM, Desal P, Serjeant GR. Climate and painful crisis of sickle-cell disease in Jamaica. Br Med J 1976;1(6001):66–68. [PubMed: 1244937]

[83]. Rezza A, Wang Z, Sennett R, Qiao W, Wang D, Heitman N, Mok KW, Clavel C, Yi R, Zandstra P, Ma'ayan A, Rendl M. Signaling Networks among Stem Cell Precursors, Transit-Amplifying Progenitors, and their Niche in Developing Hair Follicles. Cell Rep 2016;14(12):3001–3018. [PubMed: 27009580]

[84]. Richardson K, Sweatt N, Tran H, Apprey V, Uthayathas S, Taylor R, Gupta K. Significant Quantitative Differences in Orexin Neuronal Activation After Pain Assessments in an Animal Model of Sickle Cell Disease. Front Mol Biosci 2020;7:5. [PubMed: 32118032]

[85]. Ryan TM, Ciavatta DJ, Townes TM. Knockout-transgenic mouse model of sickle cell disease. Science 1997;278(5339):873–876. [PubMed: 9346487]

[86]. Rybicki AC, Benjamin LJ. Increased levels of endothelin-1 in plasma of sickle cell anemia patients. Blood 1998;92(7):2594–2596. [PubMed: 9746804]

[87]. Sadler KE, Langer SN, Menzel AD, Moehring F, Erb AN, Brandow AM, Stucky CL. Gabapentin alleviates chronic spontaneous pain and acute hypoxia-related pain in a mouse model of sickle cell disease. Br J Haematol 2019;187(2):246–260. [PubMed: 31247672]

[88]. Sadler KE, Lewis TR, Waltz TB, Besharse JC, Stucky CL. Peripheral nerve pathology in sickle cell disease mice. Pain Rep 2019;4(4):e765. [PubMed: 31579856]

[89]. Sadler KE, Moehring F, Shiers SI, Laskowski LJ, Mikesell AR, Plautz ZR, Brezinski AN, Mecca CM, Dussor G, Price TJ, McCorvy JD, Stucky CL. Transient receptor potential canonical 5 mediates inflammatory mechanical and spontaneous pain in mice. Sci Transl Med 2021;13(595).

[90]. Sadler KE, Stucky CL. Neuronal transient receptor potential (TRP) channels and noxious sensory detection in sickle cell disease. Neurosci Lett 2019;694:184–191. [PubMed: 30508569]

[91]. Sadler KE, Zappia KJ, O'Hara CL, Langer SN, Weyer AD, Hillery CA, Stucky CL. Chemokine (c-c motif) receptor 2 mediates mechanical and cold hypersensitivity in sickle cell disease mice. Pain 2018;159(8):1652–1663. [PubMed: 29697532]

[92]. Schumacher MA, Jong BE, Frey SL, Sudanagunta SP, Capra NF, Levine JD. The stretch-inactivated channel, a vanilloid receptor variant, is expressed in small-diameter sensory neurons in the rat. Neurosci Lett 2000;287(3):215–218. [PubMed: 10863033]

[93]. Scott SA. Sensory neurons: diversity, development, and plasticity: Oxford University Press, USA, 1992.

[94]. Sennett R, Wang Z, Rezza A, Grisanti L, Roitershtein N, Sicchio C, Mok KW, Heitman NJ, Clavel C, Ma'ayan A, Rendl M. An Integrated Transcriptome Atlas of Embryonic Hair Follicle Progenitors, Their Niche, and the Developing Skin. Dev Cell 2015;34(5):577–591. [PubMed: 26256211]

[95]. Servin-Vences MR, Moroni M, Lewin GR, Poole K. Direct measurement of TRPV4 and PIEZO1 activity reveals multiple mechanotransduction pathways in chondrocytes. Elife 2017;6.

[96]. Sharif B, Ase AR, Ribeiro-da-Silva A, Seguela P. Differential Coding of Itch and Pain by a Subpopulation of Primary Afferent Neurons. Neuron 2020;106(6):940–951 e944. [PubMed: 32298640]

[97]. Shiers S, Klein RM, Price TJ. Quantitative differences in neuronal subpopulations between mouse and human dorsal root ganglia demonstrated with RNAscope in situ hybridization. Pain 2020;161(10):2410–2424. [PubMed: 32639368]

[98]. Smith WR, Penberthy LT, Bovbjerg VE, McClish DK, Roberts JD, Dahman B, Aisiku IP, Levenson JL, Roseff SD. Daily assessment of pain in adults with sickle cell disease. Ann Intern Med 2008;148(2):94–101. [PubMed: 18195334]

[99]. Soga M, Izumi T, Nanchi I, Horita N, Yamamoto M, Kawasaki S, Ogawa K, Fujita M, Morioka Y. Suppression of joint pain in transient receptor potential vanilloid 4 knockout rats with monoiodoacetate-induced osteoarthritis. Pain Rep 2021;6(3):e951. [PubMed: 34396019]

[100]. Sokabe T, Fukumi-Tominaga T, Yonemura S, Mizuno A, Tominaga M. The TRPV4 channel contributes to intercellular junction formation in keratinocytes. J Biol Chem 2010;285(24):18749–18758. [PubMed: 20413591]

[101]. Sorge RE, Martin LJ, Isbester KA, Sotocinal SG, Rosen S, Tuttle AH, Wieskopf JS, Acland EL, Dokova A, Kadoura B, Leger P, Mapplebeck JC, McPhail M, Delaney A, Wigerblad G, Schumann AP, Quinn T, Frasnelli J, Svensson CI, Sternberg WF, Mogil JS. Olfactory exposure to males, including men, causes stress and related analgesia in rodents. Nat Methods 2014;11(6):629–632. [PubMed: 24776635]

[102]. Strotmann R, Harteneck C, Nunnenmacher K, Schultz G, Plant TD. OTRPC4, a nonselective cation channel that confers sensitivity to extracellular osmolarity. Nat Cell Biol 2000;2(10):695–702. [PubMed: 11025659]

[103]. Suzuki M, Mizuno A, Kodaira K, Imai M. Impaired pressure sensation in mice lacking TRPV4. J Biol Chem 2003;278(25):22664–22668. [PubMed: 12692122]

[104]. Suzuki M, Watanabe Y, Oyama Y, Mizuno A, Kusano E, Hirao A, Ookawara S. Localization of mechanosensitive channel TRPV4 in mouse skin. Neurosci Lett 2003;353(3):189–192. [PubMed: 14665413]

[105]. Swain SM, Liddle RA. Piezo1 acts upstream of TRPV4 to induce pathological changes in endothelial cells due to shear stress. J Biol Chem 2021;296:100171. [PubMed: 33298523]

[106]. Swain SM, Romac JM, Shahid RA, Pandol SJ, Liedtke W, Vigna SR, Liddle RA. TRPV4 channel opening mediates pressure-induced pancreatitis initiated by Piezo1 activation. J Clin Invest 2020;130(5):2527–2541. [PubMed: 31999644]

[107]. Talagas M, Lebonvallet N, Leschiera R, Sinquin G, Elies P, Haftek M, Pennec JP, Ressnikoff D, La Padula V, Le Garrec R, L'Herondelle K, Mignen O, Le Pottier L, Kerfant N, Reux A, Marcorelles P, Misery L. Keratinocytes Communicate with Sensory Neurons via Synaptic-like Contacts. Ann Neurol 2020;88(6):1205–1219. [PubMed: 32951274]

[108]. Tavares-Ferreira D, Shiers S, Ray PR, Wangzhou A, Jeevakumar V, Sankaranarayanan I, Cervantes AM, Reese JC, Chamessian A, Copits BA, Dougherty PM, Gereau RWt, Burton MD, Dussor G, Price TJ. Spatial transcriptomics of dorsal root ganglia identifies molecular signatures of human nociceptors. Sci Transl Med 2022;14(632):eabj8186. [PubMed: 35171654]

[109]. Thorneloe KS, Cheung M, Bao W, Alsaid H, Lenhard S, Jian MY, Costell M, Maniscalco-Hauk K, Krawiec JA, Olzinski A, Gordon E, Lozinskaya I, Elefante L, Qin P, Matasic DS, James C, Tunstead J, Donovan B, Kallal L, Waszkiewicz A, Vaidya K, Davenport EA, Larkin J, Burgert M, Casillas LN, Marquis RW, Ye G, Eidam HS, Goodman KB, Toomey JR, Roethke TJ, Jucker BM, Schnackenberg CG, Townsley MI, Lepore JJ, Willette RN. An orally active TRPV4 channel blocker prevents and resolves pulmonary edema induced by heart failure. Sci Transl Med 2012;4(159):159ra148.

[110]. Thorneloe KS, Sulpizio AC, Lin Z, Figueroa DJ, Clouse AK, McCafferty GP, Chendrimada TP, Lashinger ES, Gordon E, Evans L, Misajet BA, Demarini DJ, Nation JH, Casillas LN, Marquis RW, Votta BJ, Sheardown SA, Xu X, Brooks DP, Laping NJ, Westfall TD. N-((1S)-1-{[4-((2S)-2-{[(2,4-dichlorophenyl)sulfonyl]amino}−3-hydroxypropanoyl)-1 -piperazinyl]carbonyl}−3-methylbutyl)-1-benzothiophene-2-carboxamide (GSK1016790A), a novel and potent transient receptor potential vanilloid 4 channel agonist induces urinary bladder contraction and hyperactivity: Part I. J Pharmacol Exp Ther 2008;326(2):432–442. [PubMed: 18499743]

[111]. Tran H, Gupta M, Gupta K. Targeting novel mechanisms of pain in sickle cell disease. Blood 2017;130(22):2377–2385. [PubMed: 29187376]

[112]. Tran H, Sagi V, Jarrett S, Palzer EF, Badgaiyan RD, Gupta K. Diet and companionship modulate pain via a serotonergic mechanism. Sci Rep 2021;11(1):2330. [PubMed: 33526805]

[113]. Uhelski ML, Gupta K, Simone DA. Sensitization of C-fiber nociceptors in mice with sickle cell disease is decreased by local inhibition of anandamide hydrolysis. Pain 2017;158(9):1711–1722. [PubMed: 28570479]

[114]. Vincent L, Vang D, Nguyen J, Gupta M, Luk K, Ericson ME, Simone DA, Gupta K. Mast cell activation contributes to sickle cell pathobiology and pain in mice. Blood 2013;122(11):1853–1862. [PubMed: 23775718]

[115]. Watanabe H, Vriens J, Suh SH, Benham CD, Droogmans G, Nilius B. Heat-evoked activation of TRPV4 channels in a HEK293 cell expression system and in native mouse aorta endothelial cells. J Biol Chem 2002;277(49):47044–47051. [PubMed: 12354759]

[116]. Wu H, Bogdanov M, Zhang Y, Sun K, Zhao S, Song A, Luo R, Parchim NF, Liu H, Huang A, Adebiyi MG, Jin J, Alexander DC, Milburn MV, Idowu M, Juneja HS, Kellems RE, Dowhan W, Xia Y. Hypoxia-mediated impaired erythrocyte Lands' Cycle is pathogenic for sickle cell disease. Sci Rep 2016;6:29637. [PubMed: 27436223]

[117]. Yoneda M, Suzuki H, Hatano N, Nakano S, Muraki Y, Miyazawa K, Goto S, Muraki K. PIEZO1 and TRPV4, which Are Distinct Mechano-Sensors in the Osteoblastic MC3T3-E1 Cells, Modify Cell-Proliferation. Int J Mol Sci 2019;20(19).

[118]. Zappia KJ, Garrison SR, Hillery CA, Stucky CL. Cold hypersensitivity increases with age in mice with sickle cell disease. Pain 2014;155(12):2476–2485. [PubMed: 24953902]

[119]. Zappia KJ, Guo Y, Retherford D, Wandersee NJ, Stucky CL, Hillery CA. Characterization of a mouse model of sickle cell trait: parallels to human trait and a novel finding of cutaneous sensitization. Br J Haematol 2017;179(4):657–666. [PubMed: 29027199]

[120]. Zhang Y, Wang YH, Ge HY, Arendt-Nielsen L, Wang R, Yue SW. A transient receptor potential vanilloid 4 contributes to mechanical allodynia following chronic compression of dorsal root ganglion in rats. Neurosci Lett 2008;432(3):222–227. [PubMed: 18206306]

[121]. Zhao P, Lieu T, Barlow N, Metcalf M, Veldhuis NA, Jensen DD, Kocan M, Sostegni S, Haerteis S, Baraznenok V, Henderson I, Lindstrom E, Guerrero-Alba R, Valdez-Morales EE, Liedtke W, McIntyre P, Vanner SJ, Korbmacher C, Bunnett NW. Cathepsin S causes inflammatory pain via biased agonism of PAR2 and TRPV4. J Biol Chem 2014;289(39):27215–27234. [PubMed: 25118282]

[122]. Zhao P, Lieu T, Barlow N, Sostegni S, Haerteis S, Korbmacher C, Liedtke W, Jimenez-Vargas NN, Vanner SJ, Bunnett NW. Neutrophil Elastase Activates Protease-activated Receptor-2 (PAR2) and Transient Receptor Potential Vanilloid 4 (TRPV4) to Cause Inflammation and Pain. J Biol Chem 2015;290(22):13875–13887. [PubMed: 25878251]

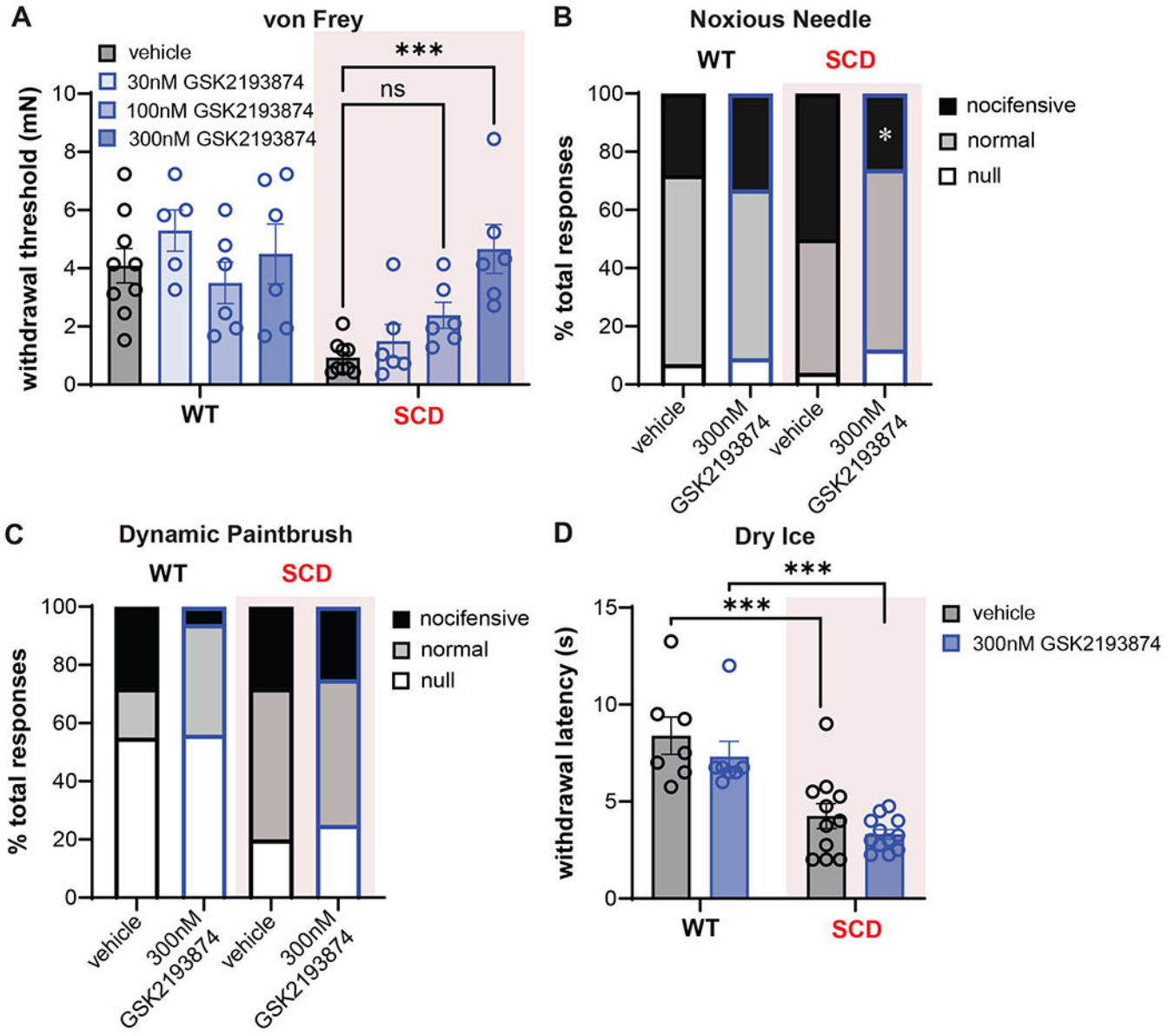

Figure 1. Blockade of TRPV4 alleviates punctate, not dynamic, mechanical hypersensitivity in SCD mice.

(A) Transgenic Townes SS (SCD) mice that received injections of vehicle into the plantar hind paw demonstrated marked sensitization on the von Frey test relative to Townes AA controls (WT). Blockade of TRPV4 with 300nM of GSK2193874 significantly increased withdrawal thresholds of SCD mice, suggesting TRPV4 plays a role in mechanical hypersensitivity associated with SCD (two-way ANOVA, significant main effect of genotype $F_{1,45} = 18.41$, $P < 0.0001$, significant main effect of GSK2193874 $F_{3,45} = 4.0$, $P < .05$, significant interaction $F_{3,45} = 3.854$, $P < .01$; Bonferroni multiple comparison test SCD vehicle vs SCD 300nM GSK2193874 ***$P = 0.0003$). (B) Chi-square analysis indicated statistically different types of behavioral responses to needle stimulation in SCD mice following TRPV4 inhibition (300nM GSK2193874; $\chi^2_{(6)} = 15.09$, *$P = .0196$; Fisher's exact SCD vehicle vs. SCD GSK2193874 of nocifensive responses *$P = .0126$). (C) Chi-

square analysis revealed statistically different types of behavioral responses to paintbrush hind paw stimulation ($\chi^2_{(6)} = 26.88$, ***$P = .0002$), but no significant effect of TRPV4 blockade (300nM GSK2193874) on response classification for WT or SCD mice. (D) Relative to controls, SCD mice display cold allodynia that persists following blockade of TRPV4 (300nM of GSK2193874; two-way ANOVA, significant main effect of genotype $F_{1,33} = 40.37$, $P < 0.0001$, non-significant effect of GSK2193874 $F_{1,33} = 2.452$, $P = 0.1269$, nonsignificant interaction $F_{1,33} = 0.0109$, $P = 0.9175$). Data are percent of total (B, C) or mean ± SEM (A, D).

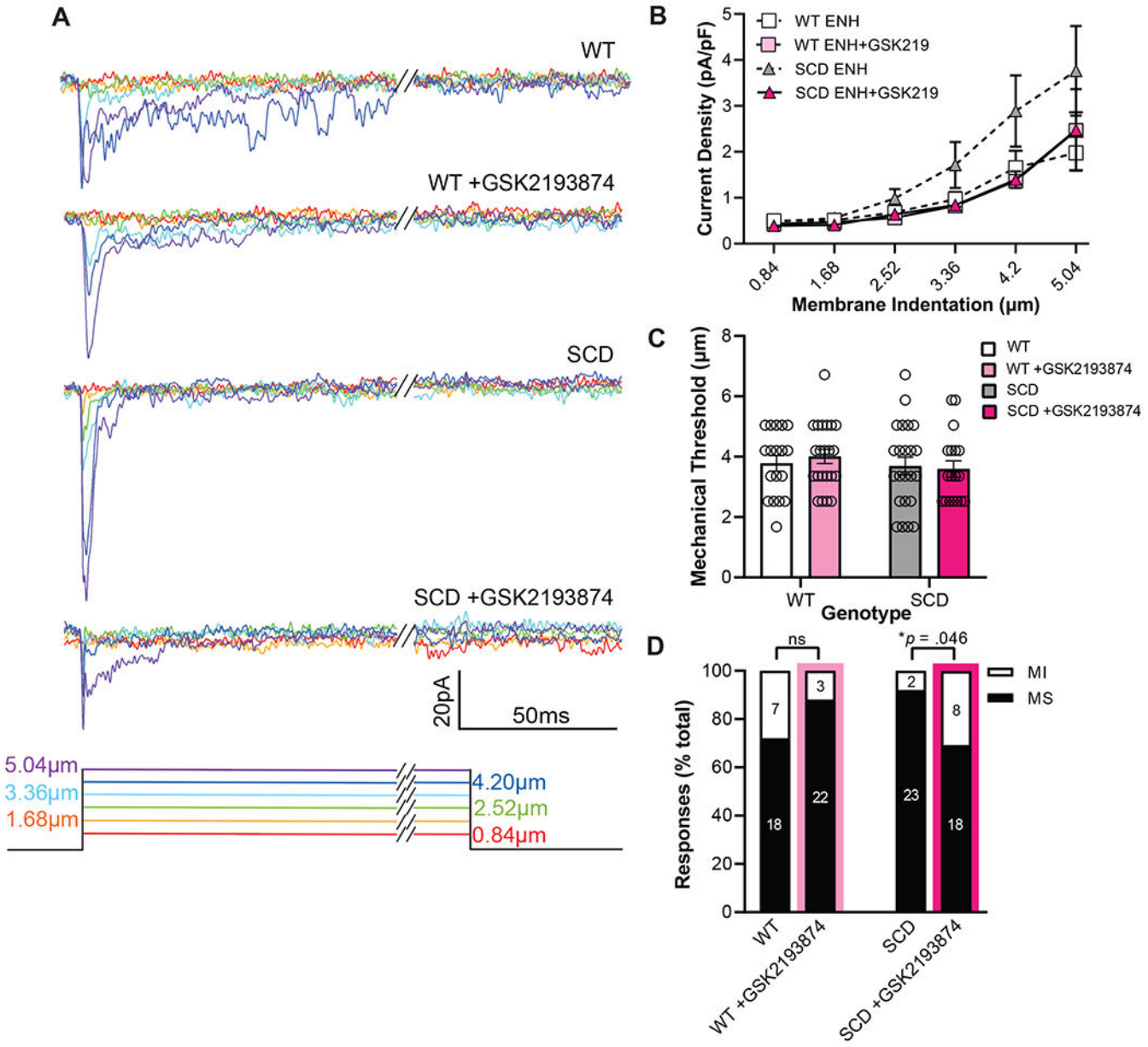

Figure 2. TRPV4 blockade reduces the mechanical sensitivity of small diameter DRG neurons from SCD mice.

(A) Representative mechanically evoked current traces from small diameter DRG neurons shown separately for each treatment group. (B) Mechanical current densities in response to stepwise increases of mechanical stimulation in the presence of extracellular normal HEPES (ENH) recording bath or recording bath containing the TRPV4 antagonist (300nM GSK2193874). Current densities remained unaffected by genotype or treatment (3-way mixed ANOVA significant within-subjects effect of stimulation $F_{(1.3,85.1)} = 29.56$, ****$P < .0001$, non-significant main effect of genotype $F_{(1,67)} = .926$, $P = .34$, non-significant main effect of treatment $F_{(1,67)} = 2.1$, $P = .15$, non-significant interaction between genotype and treatment $F_{(1,67)} = 1.36$, $P = .25$, non-significant interaction between stimulation and treatment $F_{(1.3,85.1)} = 1.06$, $P = .323$, non-significant interaction between stimulation and

genotype $F_{(1.3,85.1)} = 1.12$, $P = .31$). (C) Mechanical current thresholds were unaffected by genotype or treatment (Kruskal-Wallis$_{(3)} = 1.603$, $P = .659$). (D) 300nM GSK2193874 treatment significantly increased the proportion of mechanically insensitive (MI) neurons from SCD mice ($\chi^2_{(1)} = 4.192$, $^*P = .041$), suggesting TRPV4 blockade reduces mechanical sensitivity in these neurons. Data are mean ± SEM (B, C), or percent of total responses (D).

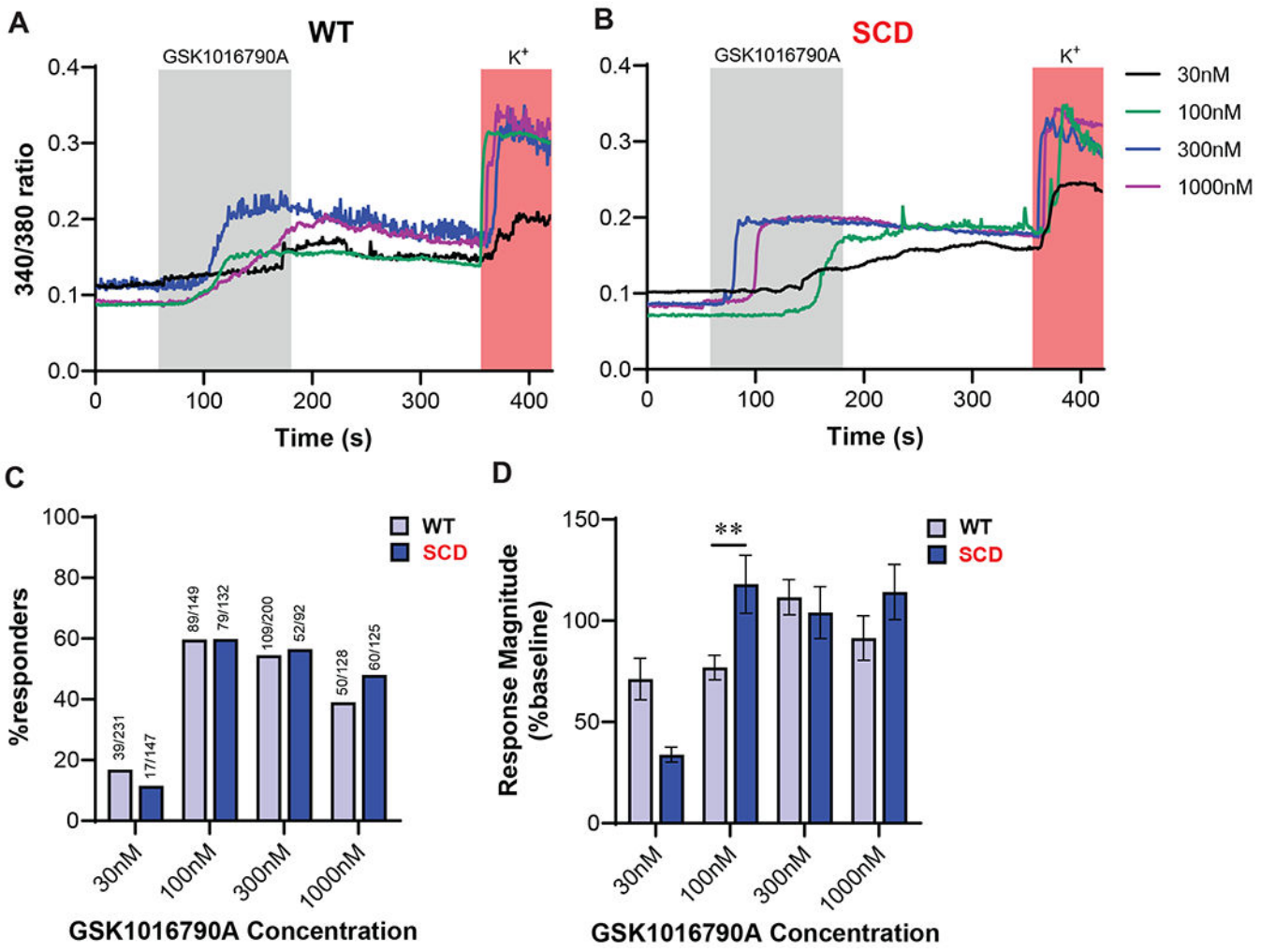

Figure 3. Effect of TRPV4 activation on calcium responses of small diameter DRG neurons from SCD mice.

(A, B) Representative calcium responses of small diameter DRG neurons isolated from WT (A) and SCD mice (B) in response to a 2 min application of 30nM, 100nM, 300nM, or 1000nM of the TRPV4 agonist GSK1016790A followed by 1 min application of 50 mM KCl. (C) While more DRG neurons responded to higher concentrations of the TRPV4 agonist ($\chi^2_{(3)} = 16.41$, $^{***}P < .001$), statistically equivalent proportions of neurons from each genotype responded to each concentration of GSK1016790A used (Fisher's Exact test WT 30nM vs SCD 30nM $P = .1561$, WT 100nM vs SCD 100nM $P = .889$, WT 300nM vs SCD 300nM $P = .801$, WT 1000nM vs SCD 1000nM $P = .1645$). (D) In response to 100nM GSK1016790A, small DRG neurons from SCD mice display significantly elevated calcium response magnitudes relative to small DRG neurons from WT mice (2-way ANOVA significant main effect of GSK1016790A concentration $F_{(3,487)} = 4.628$, $^{**}P < .01$, non-significant main effect of genotype $F_{(1,487)} = .252$, $P = .616$, significant interaction effect $F_{(3,487)} = 3.279$, $^{*}P = .021$, Bonferroni multiple comparison test WT 100nM vs SCD 100nM $^{**}P < .01$). Data are percent of total responders (C) or mean ± SEM (D).

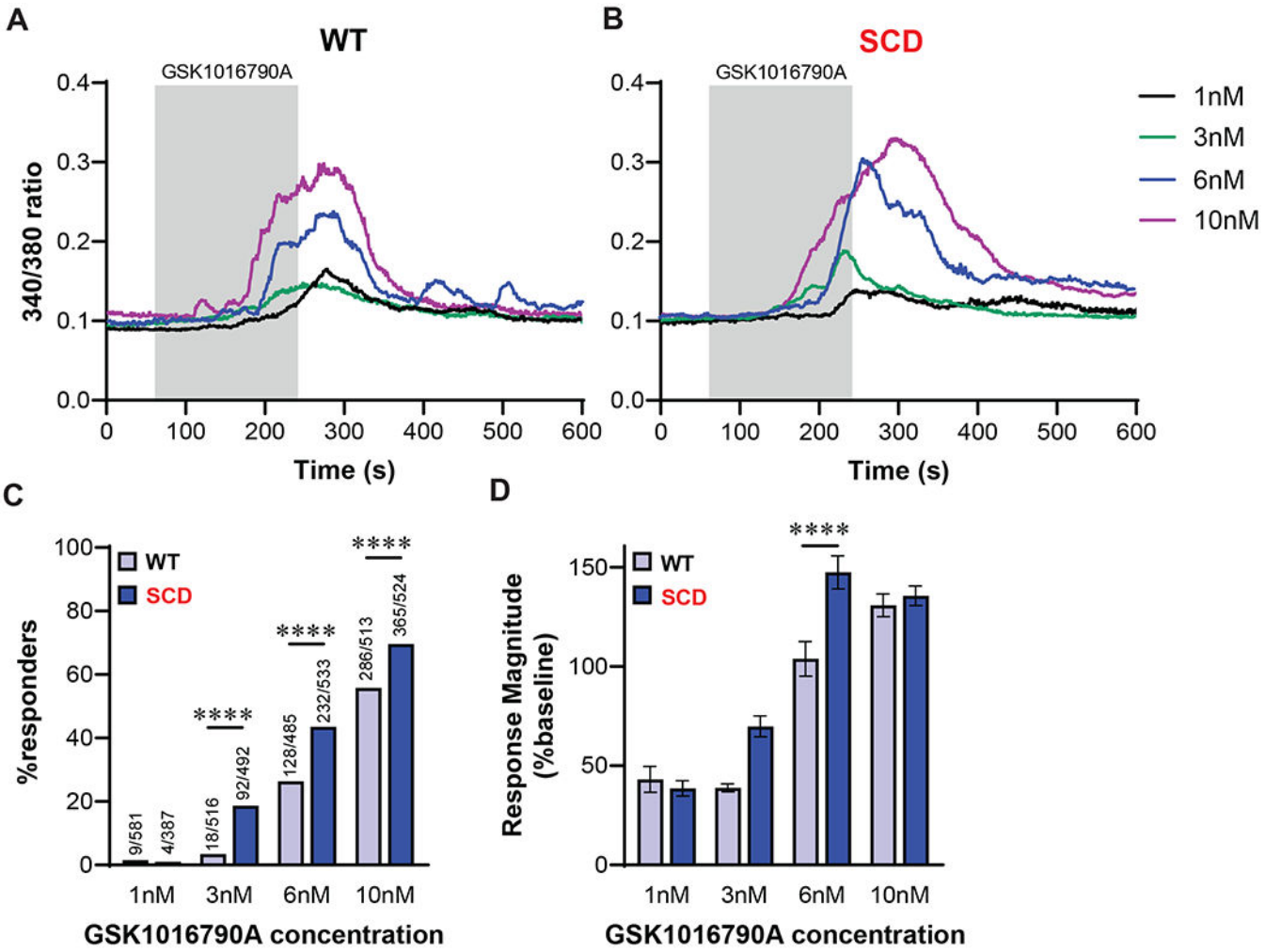

Figure 4. Keratinocytes from SCD mice display sensitized calcium responses to a TRPV4 agonist.

(A, B) Representative calcium responses of keratinocyte isolated from WT or SCD mice (B) in response to a 3 min application of 1nM, 3nM, 6nM, or 10nM of the TRPV4 agonist GSK1016790A. (C) Significantly more keratinocytes from SCD mice responded to GSK1016790A at 3nM, 6nM, and 10nM concentrations relative to keratinocytes from WT mice; statistically equivalent proportions of keratinocytes from each genotype responded to 1nM GSK1016790A ($\chi^2_{(3)} = 37.17$, $P < .0001$; Fisher's Exact test WT 3nM vs SCD 3nM ****$P < .0001$, WT 6nM vs SCD 6 nM ****$P < .0001$, WT 10nM vs SCD 10nM ****$P < .0001$). (D) In response to 6nM GSK1016790A keratinocytes from SCD mice displayed significantly elevated calcium response magnitudes relative to keratinocytes from WT mice (2-way ANOVA significant main effect of GSK1016790A concentration $F_{(3,1126)} = 14.396$, $P < .0001$, non-significant main effect of genotype $F_{(1,1126)} = 1.248$, $P = .264$, significant interaction effect $F_{(3,1126)} = 3.006$, $P = .029$; Bonferroni multiple comparison test WT 6nM vs SCD 6nM ****$P < .0001$). Data are percent of total responders (C) or mean ± SEM (D).

Table 1.

Basic membrane and action potential properties of small diameter DRG neurons isolated from SCD mice or WT controls recorded in ENH alone or ENH containing 300nM GSK2193874.

Group (# of cells)	RMP (mV) †	C_m (pF)	rheobase (pA)	AP_{thresh} (mV)*	AP_{amp} (mV)**	AP_{width} (ms)
WT (25)	−60.1 ± 3.6	25.2 ± 1.8	268.8 ± 34.4	−19.2 ± 1.6	58.4 ± 2.8	2.13 ± 0.12
WT +GSK2193874 (25)	−50.8 ± 1.6	24.6 ± 1.4	294.6 ± 66.3	−20.5 ± 1.2	62.9 ± 1.9	2.01 ± 0.12
SCD (25)	−54.5 ± 2.3	28.4 ± 2.2	380.4 ± 87.7	−23.5 ± 1.4	65.0 ± 1.9	2.06 ± 0.15
SCD +GSK2193874 (26)	−53.3 ± 1.9	28.1 ± 2.4	323.5 ± 69.8	−22.7 ± 0.9	67.0 ± 1.2	2.25 ± 0.15

Values are mean ± SEM.

† $P < .05$ main effect of GSK2193874;

* $P < .05$ main effect of genotype;

** $P < .01$ main effect of genotype; n = 11-16 mice.

RMP, resting membrane potential; C_m, cell membrane capacitance; rheobase, threshold current required to elicit an action potential; AP_{thresh}, action potential threshold; AP_{amp}, action potential amplitude; AP_{width}, action potential half-width.

Table 2.

Basic membrane and action potential properties of large diameter DRG neurons isolated from SCD mice or WT controls treated with ENH alone or ENH containing 300nM GSK2193874.

Group (# of cells)	RMP (mV)†††	C_m (pF)	rheobase (pA)†	AP_{thresh} (mV)	AP_{amp} (mV)	AP_{width} (ms)
WT (28)	−69.6 ± 1.0	59.5 ± 5.7	1428.9 ± 160.2	−26.5 ± 1.6	70.5 ± 2.3	1.1 ± .07
WT +GSK2193874 (28)	−64.2 ± 0.8	45.4 ± 2.8	1392.9 ± 167.6	−27.7 ± 1.2	67.9 ± 2.4	1.2 ± .07
SCD (31)	−67.7 ± 0.6	48.2 ± 3.8	1605.9 ± 129.2	−27.2 ± 1.2	69.2 ± 1.9	1.1 ± .08
SCD +GSK2193874 (30)	−63.6 ± 0.6	48.5 ± 2.7	1010.3 ± 96.8§§	−28.7 ± 1.2	70.3 ± 1.8	1.2 ± .07

Values are mean ± SEM.

$^{\dagger}P < .05$ or

$^{\dagger\dagger\dagger}P < .001$ main effect of GSK219;

$^{\S\S}P < .01$ versus SCD ENH; n = 7-12 mice.

RMP, resting membrane potential; C_m, cell membrane capacitance; rheobase, threshold current required to elicit an action potential; AP_{thresh}, action potential threshold; AP_{amp}, action potential amplitude; AP_{width}, action potential half-width.